Ceramics International 33 (2007) 269–272

CERAMICS
INTERNATIONAL

www.elsevier.com/locate/ceramint

Effect of zirconia addition on dielectric loss and microstructure of aluminum nitride ceramics

Shoichi Kume *, Masaki Yasuoka, Naoki Omura, Koji Watari

National Institute of Advanced Industrial Science and Technology (AIST), 2266-98 Anagahora,
Shimoshidami, Moriyama-ku, Nagoya 463-8560, Japan

Received 12 July 2005; received in revised form 27 July 2005; accepted 19 September 2005

Abstract

The effects of sintering additives on dielectric loss tangent of AlN ceramics have been investigated. Different amounts of Y_2O_3 and ZrO_2 were added as sintering additives to AlN powder and pressureless sintering was performed at 1900 °C for 2 h in a flowing nitrogen atmosphere. ZrN phase was detected in AlN ceramics when ZrO_2 addition was more than 0.1 mol.%. Densification behavior of both Y_2O_3 and ZrO_2 doped AlN ceramics was found to be a little complicated, however addition of ZrO_2 was effective in the densification of the AlN ceramics. tan δ is found to increase from less than 1×10^{-3} to around 6×10^{-3} when ZrO_2 content was more than 0.1 mol.%.

Keywords: C. Dielectric properties; D. Y_2O_3; D. ZrO_2; AlN

1. Introduction

Recent advancements in substrate and package materials for integrated circuits (ICs) require more intricate plasma devices such as plasma etching devices and plasma CVD devices using microwaves above 1×10^9 Hz (1 GHz) for machining [1–4]. In plasma devices, components such as microwave windows, protective plates, clamps and electrostatic chucks are regularly exposed to plasma. To perform their functions, these components must not only be able to withstand fluorinated reaction gases, but they must also have high heat dissipation, insulation properties and a low dielectric loss tangent (tan δ). For a microwave window, a material with excellent dielectric loss where tan δ is of the order of 3×10^{-3} or less is required [5]. Materials having a low tan δ include alumina [6], sapphire [6] and silicon nitride [7]. However, alumina and sapphire have relatively low thermal conductivity, whereas the ability of silicon nitride to withstand fluorinated reaction gases is low. Hence, these materials cannot be effectively used for the above applications.

AlN is found to be a good candidate material for these applications, since it offers high thermal conductivity (170–270 W m^{-1} K^{-1}) [8–11], high insulating properties and high withstanding capacity for fluorinated gases [12].

The tan δ is affected by intrinsic and extrinsic dielectric losses. The intrinsic loss depends on the crystal structure and shows the minimum value in a pure and perfect single crystal. On the other hand, the extrinsic loss is associated with imperfections in the crystal structure, such as the grain boundary, impurities, lattice defects, dislocations, electrical conductivity and residual stresses [13]. Therefore, reducing these imperfections in the microstructure is necessary to decrease tan δ.

However, there have been few reports regarding the effects of the above imperfections on tan δ at GHz and higher frequencies [14]. Hence, we have attempted to investigate the effects of cooling processes [15,16] followed by sintering, as well as the effects of addition of MgO [17], Mg_3N_2 [18] and TiO_2 [19] as tertiary phases to an AlN–Y_2O_3 system to study the variation in tan δ of AlN ceramics. The tan δ decreased significantly by adding TiO_2 [19], even if it is expected that TiN formed by the reaction of AlN and TiO_2 might increase the tan δ value.

Therefore, the objective of this study is to evaluate the effect of ZrO_2 addition on tan δ of AlN ceramics.

---

* Corresponding author. Tel.: +81 52 736 7158; fax: +81 52 736 7405.
E-mail address: s.kume@aist.go.jp (S. Kume).

0272-8842/$32.00 © 2005 Elsevier Ltd and Techna Group S.r.l. All rights reserved.
doi:10.1016/j.ceramint.2005.09.015

2. Experimental procedure

AlN powder (MAN-2, Mitsui Chemicals, Tokyo, Japan) was used as the starting material. 0.5 and 1 mol.% Y_2O_3 (Daiichi Kigenso Kagaku Kogyo Co. Ltd., Osaka, Japan) and 0, 0.1, 0.5 and 1 mol.% ZrO_2 (TZ-3Y, Tosoh corporation, Osaka, Japan) were added to AlN powder as sintering additives. These powders were mixed in ethanol using a planetary ball milling device (Pulverisette 6, Fritsch Japan, Tokyo, Japan), dried and made into pellets of 16 mm diameter and 5 mm thickness by uniaxial molding, followed by cold isostatic pressing at a pressure of 100 MPa. The cold isostatically pressed AlN–Y_2O_3–ZrO_2 compacts were pressureless-sintered at 1900 °C for 2 h in a flowing nitrogen atmosphere. Following the sintering, AlN samples were cooled at a rate of 1 °C min^{-1} from 1900 to 1750 °C, at a rate of 30 °C min^{-1} to annealing temperature of 970 °C and annealed for 4 h and then cooled at a rate of 30 °C min^{-1}. The bulk densities of the AlN samples obtained were measured using Archimedes' method. To measure tan δ of the AlN samples, machining and polishing were performed on the rectangular solids (7.0 mm × 5.0 mm × 3.5 mm). Dielectric loss was measured at 0.125 GHz intervals within the range of the R band (26.5–40.0 GHz) at room temperature by the full two-port S-parameter measurement with an hp85071C application software using an HP 8722ES S-Parameter Network Analyzer. Crystalline phases in the AlN samples were identified by X-ray diffraction (XRD) analysis. Fracture surfaces of AlN samples were observed using scanning electron microscopy (SEM).

3. Results and discussions

3.1. XRD analysis

There was no significant difference in XRD patterns of sintered AlN samples added with Y_2O_3 between 0.5 and 1.0 mol.%. Fig. 1 shows the XRD profiles of sintered AlN samples obtained by adding 1 mol.% Y_2O_3 and various amounts of ZrO_2 as typical results. Though $Al_5Y_3O_{12}$ ($5Al_2O_3/3Y_2O_3$: YAG) phase was detected clearly in AlN–Y_2O_3 system, addition of 0 and 0.1 mol.% ZrO_2, leads to the formation of a YAG phase and found to vanish when more than 0.5 mol.% ZrO_2 is added. On the other hand, ZrN phase have been detected by the addition of 0.1 mol.% ZrO_2 to AlN–Y_2O_3, while unknown peaks have been observed when ZrO_2 content is increased to 1 mol.%. The formation of ZrN phase might be occurring due to the following [20].

$$\lambda ZrO_2 + 2AlN \rightarrow Al_2O_3 + \lambda ZrN + \left(1 - \frac{\lambda}{2}\right)N_2 + \left(\lambda - \frac{3}{2}\right)O_2 \quad (\lambda : 1.5 \text{ or } 2.0) \qquad (1)$$

According to Eq. (1), Al_2O_3 phase is also formed as a byproduct with increased formation of ZrN phase. However, even if the formation of Al_2O_3 is increased according to above reaction in an AlN sample, the stoichiometric composition of YAG phase is retained. This is in accordance with the standard Y_2O_3–Al_2O_3 phase diagram [21]. Furthermore, no other YAG–ZrO_2 mixed phases have been observed [22]. However, in AlN samples obtained by the addition of more than 0.5 mol.% ZrO_2, Al_2O_3 as well as YAG has not been observed. Furthermore, peaks of unknown phase (*X*) differ with those of fluorite type zirconia–yttria solid solution, which is a product from Al_2O_3–Y_2O_3–ZrO_2 system [23,24].

On the other hand, Zr–Al–O–N (or ZrAlON) phase was not evaluated in this study. Since Zr–Al–O–N compound is a superlattice of ZrN the strongest X-ray lines of ZrN and Zr–Al–O–N phase overlap [20,25]. Zr–Al–O–N phase formation may however be observed according to the following equations [25].

$$5AlN + 6ZrO_2 \rightarrow Al_5Zr^{3+}_{6x} + Zr^{4+}_{4-6x}O_8N_{5-2x} + xN_2\uparrow \quad 0 \le x \le 0.22 \qquad (2)$$

$$Al_2O_3 + yZrN \rightarrow Al_2Zr_y^{3+}O_3N_x \qquad 1.7 \le y \le 3.15 \qquad (3)$$

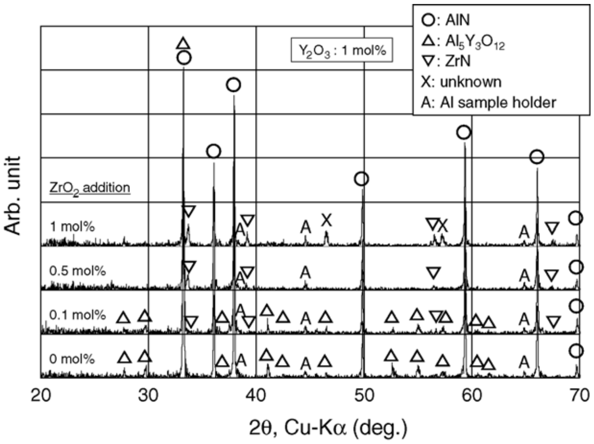

Fig. 1. Typical XRD patterns of AlN ceramics.

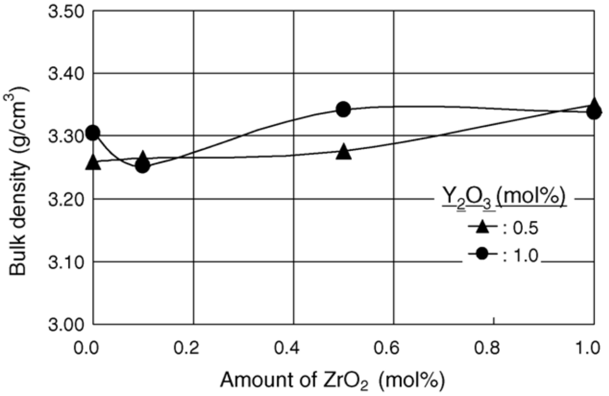

Fig. 2. Relationship between bulk density and amount of ZrO_2.

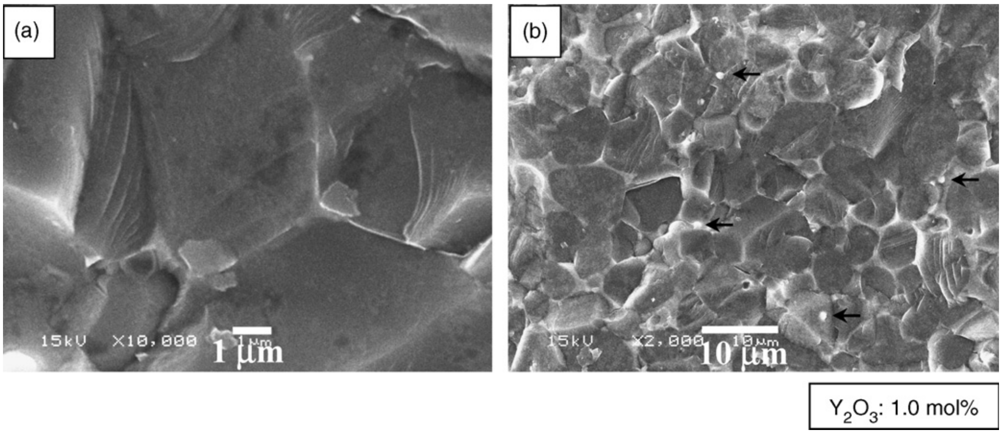

Fig. 3. SEM photographs of fracture surfaces. High magnification (a), and low magnification (b). Arrows indicate ZrN grains in (b).

$$5\mathrm{AlN} + 6\mathrm{ZrO_2} + \mathrm{Al_2O_3} + y\mathrm{ZrN} \rightarrow \mathrm{Al_7Zr^{3+}_{6x+y}Zr^{4+}_{4-6x}O_{11}N_{5-2x+y}} + x\mathrm{N_2}\uparrow \quad 0 \le z \le \frac{1}{2}x - \frac{5}{8}, \quad 1.4 \le y \le 6.5 \qquad (4)$$

According to above Eqs. (2–4), Zr–Al–O–N phases would be formed not only by the reaction of AlN and ZrO_2 but also by the mutual reactions of their reaction products. In these cases, no identification of Al_2O_3 in AlN samples obtained by adding ZrO_2 of 1 mol.% is acceptable. The reason for the absence of YAG phase in the AlN–Y_2O_3–1 mol.% ZrO_2 is still not clear. Hence, further detailed investigation is necessary to study the phase formation in the Al–Y–Zr–O–N system.

3.2. Density

Fig. 2 demonstrates the relationship between the effect of ZrO_2 addition on the bulk density of AlN ceramics. The amount of Y_2O_3 is indicated in the figure. The AlN ceramics with 0.5 and 1 mol.% Y_2O_3 and without ZrO_2 showed densities of 3.26 and 3.3 g cm^{-3}. Densification behavior of AlN ceramics depending on the amount of ZrO_2 is a little complicated. Addition of ZrO_2 (except 0.1 mol.%) was effective in the densification of the AlN ceramics. Komeya et al. reported that ZrO_2 alone was not effective in the densification of AlN [26]. Hence, composition of AlN (including Al_2O_3 as an impurity for AlN)–Y_2O_3–ZrO_2 might cause the complex densification behavior of AlN ceramics.

3.3. Microstructure

Fig. 3 shows the SEM photographs of fracture surfaces of the AlN ceramic (ZrO_2: 1.0 mol.%) with high magnification (×10,000) (a) and low magnification (×2000) (b). As shown in Fig. 3(b), ZrN (indicated with arrows) shows a grain size of 1 μm or less while AlN shows grain size in the range 3–10 μm, respectively. Unclear grain boundary phase can also be observed surrounding AlN grain, indicating the unknown phases. These unknown phases are also been detected by XRD. Due to the effect of slow-cooling followed by sintering, dihedral angle of some AlN grains is found to increase as shown in Fig. 3(a). No pore and defect are observed in both microstructures as shown in Fig. 3(a) and (b). Therefore, this AlN sample might be fully densified according to the SEM observations.

3.4. Dielectric loss

Fig. 4 shows the relationship between the percentage of ZrO_2 addition and the dielectric loss tangent (tan δ) at 28 GHz Gyrotron band. The values shown in the figure are average values of 12 points obtained by four measurements in the range of 28.000 ± 0.125 GHz for each sample. The error bars in the figure show standard deviation around the average values. Both AlN ceramics including 0.5 and 1.0 mol.% Y_2O_3 without ZrO_2 addition have tan δ less than 1.0×10^{-3}. tan δ values of AlN–Y_2O_3 was increased clearly with increasing ZrO_2 and were found to be around 6×10^{-3} when 1.0 mol.% ZrO_2 has been added. Hence, it was revealed that the addition of ZrO_2 aggravated tan δ, due to the forming of ZrN.

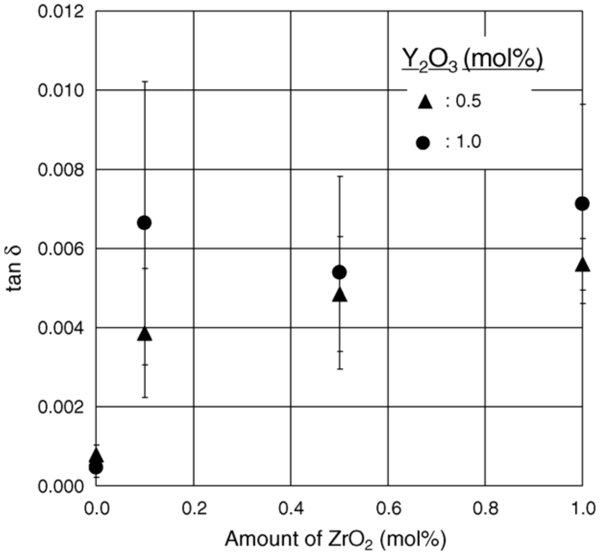

Fig. 4. Relationship between tan δ and amount of ZrO_2.

4. Conclusions

Attempts have been made to clarify the effect of addition of ZrO_2 (0, 0.1, 0.5 and 1 mol.%) to $AlN–Y_2O_3$ system with respect to $\tan\delta$ of AlN ceramics. The samples were pressureless-sintered at 1900 °C for 2 h in a flowing nitrogen atmosphere. The results are as follows:

1. ZrN phase was identified from XRD when the addition of ZrO_2 was more than 0.1 mol.%.
2. Densification behavior of AlN ceramics depending on the amount of ZrO_2 is a little complicated, but addition of ZrO_2 was effective in the densification of the AlN ceramics.
3. An increase in $\tan\delta$ from less than 1×10^{-3} to 6×10^{-3} has been observed when the ZrO_2 content is more than 0.1 mol.%. Addition of higher amount of ZrO_2 (>0.1 mol.%) aggravated the $\tan\delta$ value of AlN due to the formation of ZrN phase.

Acknowledgments

We greatly acknowledge Dr. T. Shimada (NEOMAX Co., LTD., Osaka, Japan), Professor H. Ogawa and Professor A. Kan (Meijo University, Japan) and Dr. W. Chen, Dr. N.F. Gao, Dr. M. Polat and Dr. P. Vasudev (AIST, Nagoya, Japan) for valuable discussions.

References

[1] R. Heidinger, S. Nazare, Influence of porosity on the dielectric properties of AlN in the range of 30–40 GHz, Powder Metall. Int. 20 (6) (1988) 30–32.

[2] M. González, A. Ibarra, The dielectric behavior of commercial polycrystalline aluminium nitride, Diamond Relat. Mater. 9 (2000) 467–471.

[3] R.C. Enck, J.H. Harris, R.A. Youngman, T.S. Nemecek (Carborundum Corp.), US Patent 6 017 485, 25 January 2000.

[4] I.P. Fesenko, M.A. Kuzenkova, Low dielectric loss ceramics of AlN fine and nanopowders, Powder Metall. Metal Ceram. 41 (11–12) (2002) 567–569.

[5] K. Nishizono, U. Oh (Kyocera Co. Ltd.), Japan kokai tokkyo koho, Toku-kai 2001-181049, 3 July 2001.

[6] N.M. Alford, J. Breeze, X. Wang, S.J. Penn, S. Dalla, S.J. Webb, N. Ljepojevic, X. Aupi, Dielectric loss of oxide single crystals and polycrystalline analogues from 10 to 320 K, J. Euro. Ceram. Soc. 21 (15) (2001) 2605–2611.

[7] K. Tajima, H. Uchimura (Kyocera Co. Ltd.), Japan kokai tokkyo koho, Toku-kai-hei8-295567, 12 November 1996.

[8] K. Watari, H.J. Hwang, M. Toriyama, S. Kanzaki, Effective sintering aids for low-temperature sintering of AlN ceramics, J. Mater. Res. 14 (4) (1999) 1409–1417.

[9] T.B. Jackson, A.V. Virkar, K.L. More, R.B. Dinwiddie Jr., R.A. Culter, High-thermal-conductivity aluminum nitride ceramics: the effect of thermodynamic, kinetic, and microstructural factors, J. Am. Ceram. Soc. 80 (6) (1997) 1421–1435.

[10] G. Pezzotti, A. Nakahira, M. Tajika, Effect of extended annealing cycles on the thermal conductivity of AlN/Y_2O_3 ceramics, J. Euro. Ceram. Soc. 20 (9) (2000) 1319–1325.

[11] H. Nakano, K. Watari, H. Hayashi, K. Urabe, Microstructural characterization of high-thermal-conductivity aluminum nitride ceramic, J. Am. Ceram. Soc. 85 (12) (2002) 3093–3095.

[12] T. Koyama, M. Ishii (Taiheiyo cement Co. Ltd.), Japan kokai tokkyo koho, Toku-kai 2001-233676, 28 August 2001.

[13] S.J. Penn, N.M. Alford, A. Templeton, X. Wang, M. Xu, M. Reece, K. Schrapel, Effect of porosity and grain size on the microwave dielectric properties of sintered alumina, J. Am. Ceram. Soc. 80 (7) (1997) 1885–1888.

[14] T. Koyama, M. Iguchi, M. Ishii, Lowering of dielectric loss in AlN ceramics, Taiheiyo Semento Kenkyu Hokoku 142 (2002) 78–82.

[15] S. Kume, M. Yasuoka, N. Omura, K. Watari, Annealing effect on dielectric property of AlN ceramics, J. Euro. Ceram. Soc., in press.

[16] S. Kume, M. Yasuoka, N. Omura, K. Watari, Effects of annealing on dielectric loss and microstructure of aluminum nitride ceramics, J. Am. Ceram. Soc. 88 (1) (2005) 3229–3231.

[17] S. Kume, M. Yasuoka, N. Omura, K. Watari, Effects of MgO addition on the density and dielectric loss of AlN ceramics sintered in presence of Y_2O_3, J. Euro. Ceram. Soc. 25 (12) (2005) 2791–2794.

[18] S. Kume, M. Yasuoka, N. Omura, K. Watari, Dielectric properties of sintered aluminum nitride, Int. J. Refract. Met. Hard Mater. 23 (2005) 382–385.

[19] S. Kume, M. Yasuoka, N. Omura, K. Watari, Effect of additives on dielectric loss of AlN ceramics, Key Eng. Mater., in press.

[20] C. Toy, E. Savrun, Novel composites in the aluminum nitride-zirconia and -hafnia systems, J. Euro. Ceram. Soc. 18 (1) (1998) 23–29.

[21] T. Noguchi, M. Mizuno, Kogyo Kogaku Zashi 70 (1967) 839 (Phase diagrams for ceramists Fig. 4370).

[22] J.M. Calderon-Moreno, M. Yoshimura, $Y_3Al_5O_{12}$(YAG)-ZrO_2 binary eutectic composites obtained by melt quenching, Mater. Sci. Eng. A 375–377 (2004) 1250–1254.

[23] J.M. Calderon-Moreno, M. Yoshimura, Effect of melt quenching on the subsolidus equilibria in the ternary system Al_2O_3-$Y_3Al_5O_{12}$-ZrO_2, Solid State Ionics 141–142 (2001) 343–349.

[24] J.M. Calderon-Moreno, M. Yoshimura, Rapidly solidified eutectic composites in the system Al_2O_3-Y_2O_3-ZrO_2: ternary regions in the subsolidus diagram, Solid State Ionics 154–155 (2002) 311–317.

[25] T. Stoto, J.C. Doukhan, A. Mocellin, Analytical electron microscopy investigation of the AlN-ZrO_2 system: identification of a quaternary Zr-Al-O-N phase, J. Am. Ceram. Soc. 72 (8) (1989) 1453–1457.

[26] K. Komeya, H. Inoue, A. Tsuge, Effect of various additives on sintering of aluminum nitride, Yogyo-Kyokai-Shi 89 (6) (1981) 58–64.